

# Standard line broadening impact theory for hydrogen including penetrating collisions

S. Alexiou and A. Poquérusse

*Physique Atomique dans les Plasmas Denses-LULI, Unité Mixte No. 7605 CNRS-CEA-Ecole Polytechnique-Université Paris VI,  
91128 Palaiseau cedex, France*

(Received 11 May 2005; published 17 October 2005)

In recent years there has been significant interest in the emission spectra from high-density plasmas, as manifested by a number of experiments. At these high densities short range (small impact parameter) interactions become important and these cannot be adequately handled by the standard theory, whose predictions depend on some cutoffs, necessary to preserve unitarity, the long range approximation, and to ensure the validity of a semiclassical picture. Very recently, as a result of a debate concerning the broadening of isolated ion lines, the importance of penetration of bound electron wave functions by plasma electrons has been realized. By softening the interaction, penetration makes perturbative treatments more valid. The penetration effect has now been included analytically into the standard theory. It turns out that the integrations may be done in closed form in terms of the modified Bessel functions  $K_0$  and  $K_1$ . This work develops the new theory and applies it to experimental measurements.

DOI: 10.1103/PhysRevE.72.046404

PACS number(s): 52.70.Kz, 32.70.Jz, 32.30.Jc, 32.60.+i

## I. INTRODUCTION

The modern theory of spectral line broadening [1] started with the standard separation of the broadening contributions by electrons and ions. Electrons are treated in the impact theory. This employs a second order perturbative treatment to the self-energy and a classical path trajectory to describe their motion. For the ionic contribution the quasistatic approximation was used. For both electrons and ions the emitter-perturber interaction is taken to be dipole only. This treatment is referred to as “Standard Theory”(ST) and is still used, despite problems [2], for which we now have quite good solutions. The role of ion dynamics is by now well understood so we will concentrate on electronic broadening in the impact approximation in this work. Although the field is moving forward [3,4], some fundamental problems, discussed below, remain.

The main problem with the standard electron treatment has always been the so-called strong collisions, i.e., short impact parameter collisions for which (a) perturbation theory was not valid and only unitarity-based error bounds could be computed, (b) the long range dipole/quadrupole approximation used for the interaction was questionable due to penetration by the perturbing electrons into the atomic wavefunction extent, and (c) the classical picture of point perturbers moving along predetermined classical trajectories with fixed velocities was in doubt. ST calculations are reliable to the extent that the error bound or estimate associated with the cutoffs due to the “strong” collisions is small compared to the contribution of the remainder of the phase space. We say error bounds because the contribution of strong collisions may not be computed within ST and only unitarity-based error bounds may be given. Note that these error bounds are not small for high densities. The cutoffs referred to mainly translate to a minimum impact parameter  $\rho_{min}(v)$  such that the standard treatment is valid for  $\rho > \rho_{min}(v)$  (and not valid for smaller  $\rho$ ). In the last few years it was realized [5,6] that first, penetration may be more important than

thought because the standard cutoff  $n^2 a_0 / Z$  representing the wave-function extent is too optimistic [7], at least for non-hydrogenic ions. Second, penetration softens the interaction so that perturbation theory is actually quite valid, even for collisions previously thought “strong.” However, this would have to be a *new* perturbative impact theory that properly accounts for penetration. The object of this work is to develop the ST with proper account for penetration. We will refer to this version of the ST as penetrating standard theory (PST).

## II. BRIEF THEORETICAL REVIEW

The ST expression for the self-energy (collision operator)  $\Phi$  is

$$\begin{aligned} \langle \alpha\beta | \Phi | \alpha'\beta' \rangle = & \sum_{\alpha''} \mathbf{r}_{\alpha\alpha''} \cdot \mathbf{r}_{\alpha''\alpha'} \phi(\omega_{\alpha\alpha''}, \omega_{\alpha''\alpha'}) \\ & + \sum_{\beta''} \mathbf{r}_{\beta'\beta''} \cdot \mathbf{r}_{\beta''\beta} \phi(\omega_{\beta'\beta''}, \omega_{\beta''\beta}) \\ & - \mathbf{r}_{\alpha\alpha'} \cdot \mathbf{r}_{\beta'\beta} \phi_i(\omega_{\alpha\alpha'}, \omega_{\beta'\beta}), \end{aligned} \quad (1)$$

where  $\alpha, \alpha'$  are upper level states and  $\alpha''$  is a state perturbing the upper level states. By this we mean that a collision with a plasma electron has a nonnegligible probability amplitude to cause a transition  $\alpha \rightarrow \alpha''$ . Similarly  $\beta, \beta'$  are lower level states and  $\beta''$  perturbs them. Here we deal with hydrogen only, so we employ the no-quenching approximation, i.e.,  $\alpha, \alpha', \alpha''$  have the upper level principal quantum number and  $\beta, \beta', \beta''$  have the lower level principal quantum number.  $\phi$  is essentially the velocity integrated  $a+ib$  function of ST (though in the present work the shift is identically 0 in ST, which factorizes the density matrix [8,9]). Because penetration only affects the radial integrals, the exact generalization of the ST expressions to account for penetration are given in [5] in terms of the correction factors  $C_\lambda$  (which are 1 in ST), which effectively modify the electric fields:

$$C_\lambda(R;n,l,n',l') = \frac{\int_0^R P_{nl}(r)P_{n'l'}(r)r^\lambda dr}{\int_0^\infty P_{nl}(r)P_{n'l'}(r)r^\lambda dr} + R^{2\lambda+1} \frac{\int_R^\infty dr P_{nl}(r)P_{n'l'}(r)r^{-(\lambda+1)}}{\int_0^\infty P_{nl}(r)P_{n'l'}(r)r^\lambda dr} \quad (2)$$

with  $P_{nl}$  denoting the radial wave function with principal quantum number  $n$  and orbital quantum number  $l$ ,  $R(t)$  the position of the perturber at time  $t$ , and  $\lambda$  the multipole order (1=dipole, 2=quadrupole). Note that  $C_\lambda$  is real and symmetric in the states involved. In analogy to the ST we only consider the dipole ( $\lambda=1$ ) contribution here. We note that this is still the most important contribution to broadening even in the presence of penetration. We thus deal with  $C_1$  exclusively from now on. The “direct” PST  $\phi$  is then computed as

$$\begin{aligned} \phi^{\text{PST}}(\omega_1, \omega_2) = & -\frac{2\pi e^2 n}{3\hbar^2} \int_0^\infty v f(v) dv \int \rho d\rho \int_{-\infty}^\infty dt_1 e^{i\omega_1 t_1} \\ & \times \int_{-\infty}^{t_1} dt_2 e^{i\omega_2 t_2} C_1(R(t_1); n_\alpha, l_\alpha, n_{\alpha'}, l_{\alpha'}) \\ & \times C_1(R(t_2); n_{\alpha'}, l_{\alpha'}, n_{\alpha''}, l_{\alpha''}) \mathbf{E}(t_1) \cdot \mathbf{E}(t_2) \quad (3) \end{aligned}$$

and similarly for the lower level direct term. Of course in the hydrogen case  $\omega_1 = \omega_2 = 0$  and  $n_\alpha = n_{\alpha'} = n_{\alpha''}$ . For the interference term we have

$$\begin{aligned} \phi_i^{\text{PST}}(\omega_1, \omega_2) = & -\frac{2\pi e^2 n}{3\hbar^2} \int_0^\infty v f(v) dv \int \rho d\rho \int_{-\infty}^\infty dt_1 e^{i\omega_1 t_1} \\ & \times \int_{-\infty}^\infty dt_2 e^{i\omega_2 t_2} C_1(R(t_1); n_\alpha, l_\alpha, n_{\alpha'}, l_{\alpha'}) \\ & \times C_1(R(t_2); n_{\beta'}, l_{\beta'}, n_{\beta''}, l_{\beta''}) \mathbf{E}(t_1) \cdot \mathbf{E}(t_2). \quad (4) \end{aligned}$$

With regard to the limits of the  $\rho$  integration, the upper limit  $\rho_{max}$  is taken to be of the order of the Debye length  $\lambda_D$  ( $0.68\lambda_D$  to account for the shielded Debye fields instead of the pure Coulomb fields used in ST), unless this is comparable to the interparticle spacing. The important point is that  $\rho_{max}$  is *velocity-independent*, as the ST does not deal with effects associated with the wake of a very fast perturber. The lower limit cannot be 0 in ST because perturbation theory breaks down, because the long range dipole approximation breaks down, and finally because the de Broglie wavelength of the perturber must be smaller than  $\rho_{min}$ . For the moment (we will be more precise later in this work) we note that in PST, only the last consideration is always important, as perturbation theory is always valid for  $\rho=0$  and often valid down to  $\rho=0$ . In that case and in accord with standard practice we take in the present work the limits of the  $\rho$  integration to be  $(0, 0.68\lambda_D)$ . The important point is that  $\rho_{max}$  is the same as the  $\rho_{max}$  used in the ST. Similarly, the

lower limit in the velocity integration should not be 0, but a velocity at which point the de Broglie wavelength becomes comparable to  $\rho_{max}$ . This complication is also ignored in the present work. Then the velocity integration gives a factor  $\langle v^{-1} \rangle = \sqrt{2m/\pi kT}$ .

The new  $\phi$  functions are emitter and line-dependent. In general there are four types of expressions with this general starting formula, depending on whether the imaginary exponentials may be replaced by unity (as for hydrogen and hydrogenlike lines in the no-quenching approximation) or not and on whether  $\mathbf{E}(t)$  corresponds to a straight line (neutrals) or hyperbolic (ions) trajectory. However, it does not appear to be possible to develop these expressions analytically for other cases except hydrogen, so in the other cases a fully numerical approach [5] might be preferable. For hydrogen we note that on the one hand quantal methods may have some difficulties and on the other hand, for semiclassical methods, backreaction and thresholds are not an issue.

### III. APPLICATION TO HYDROGEN

For hydrogen we have two simplifications: First we drop the imaginary exponentials: If this is not valid, then the problem reduces to the second case (nonhydrogenic neutrals). This implies that  $\phi$  is purely real. Second, we choose explicitly a straight line trajectory:

$$\mathbf{R}(t) = \boldsymbol{\rho} + \mathbf{v}t. \quad (5)$$

For the remainder of this work, we keep the notation of the previous section using  $n, n', \dots$ , although all these are the same here. The result is that

$$\begin{aligned} \phi^{\text{PST}}(\omega_1, \omega_2) = & -\frac{\pi e^4 n}{3(4\pi\epsilon_0\hbar)^2} \int_0^\infty v f(v) dv \int \rho d\rho \\ & \times I(\rho, v; n_\alpha, l_\alpha, n_{\alpha'}, l_{\alpha'}) I(\rho, v; n_{\alpha'}, l_{\alpha'}, n_{\alpha''}, l_{\alpha''}), \quad (6) \end{aligned}$$

$$I(\rho, v; n, l, n', l') = \rho \int_{-\infty}^\infty dt \frac{C_1((\rho^2 + v^2 t^2)^{1/2}; n, l, n', l')}{(\rho^2 + v^2 t^2)^{3/2}}. \quad (7)$$

The ST result is then simply ( $C_1=1$ ):  $I_{\text{ST}} = \frac{2}{\rho v}$ . For hydrogen the wave functions are known analytically in terms of the Laguerre polynomials  $L$ :

$$P_{nl} = \frac{A}{a} e^{-z/2} z^{l+1} L_{n+l}^{2l+1}(z), \quad (8)$$

with  $z = ar$ ,  $a = \frac{2}{na_0}$ ,  $A = -\sqrt{a^3 \{(n-l-1)! / 2n[(n+l)!]^3\}}$ , and hence  $C_\lambda$  may be computed analytically.

$$C_\lambda = 1 - e^{-aR(t)} p_{n+n'+\lambda}(aR(t)) \quad (9)$$

where  $p_k(x) = \sum_{i=0}^k s_i x^i$  is a polynomial of degree  $k$ . The coefficients  $s_i$  are computed in the Appendix and are rapidly decreasing functions of  $i$ .

Note that  $s_0 = s_1 = 1$  and  $s_2 = 0.5$ .  $I$  therefore has the form

$$I = \frac{2}{\rho v} [1 - \Delta(b)], \quad \Delta(b) = \sum_{i=0}^{n+n'+\lambda} s_i b^i F_{i-2}(b) \quad (10)$$

with

$$F_q(b) = \int_0^\infty du e^{-b \cosh u} (\cosh u)^q, \quad (11)$$

where  $s_i$  are the coefficients of the polynomial  $p$  defined above. All corrections due to penetration are contained in the  $\rho$ -dependent function  $\Delta(b)$ . For scaling the only relevant variable is  $b = a\rho$ . Thus, as long as the minimum impact parameter is velocity-independent (zero, as discussed above), the velocity integration may be done separately.

To proceed further, we note the following values for the function  $F_q(b)$ ,  $q = -2, \dots, n+n'+\lambda-2$ :

$$F_{-2}(b) = Ki_2(b), F_{-1}(b) = Ki_1(b),$$

$$F_0(b) = K_0(b), F_1(b) = K_1(b), \quad (12)$$

where  $K_\nu$  are modified Bessel functions and  $Ki_q$  are their integrals:

$$Ki_0(b) = K_0(b), \quad Ki_q(b) = \int_b^\infty Ki_{q-1}(x) dx \quad (13)$$

as well as the recursion relation:

$$F_{q+2}(b) = F_q(b) + \frac{(q+1)F_{q+1}(b) - qF_{q-1}(b)}{b}. \quad (14)$$

The recursion relation may be obtained as follows:

$$F_{q+2} = F_q + \int_0^\infty du e^{-b \cosh u} \cosh^q u \sinh^2 u$$

$$= F_q + \int_0^\infty d\left(\frac{e^{-b \cosh u}}{b}\right) \cosh^q u \sinh u$$

$$= F_q + \frac{1}{b} \int_0^\infty e^{-b \cosh u} d(\cosh^q u \sinh u) \quad (15)$$

since the surface terms vanish because of the  $\sinh u$  at  $b=0$ . The last integral is

$$b^{-1} \int e^{-b \cosh u} (q \cosh^{q-1} u \sinh^2 u + \cosh^{q+1} u)$$

$$= b^{-1} \int e^{-b \cosh u} [q \cosh^{q-1} u (\cosh^2 u - 1) + \cosh^{q+1} u]$$

$$= b^{-1} [(q+1)F_{q+1}(b) - qF_{q-1}(b)]. \quad (16)$$

For the numerical implementation we defined  $H_p(b) = b^p F_p(b)$  in terms of

$$H_0(b) = K_0(b),$$

$$H_1(b) = bK_1(b),$$

$$H_2(b) = bK_1(b) + b^2K_0(b),$$

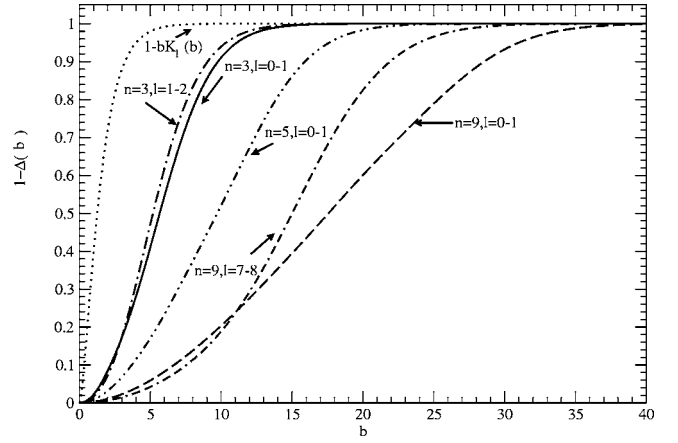


FIG. 1. Plots of  $1 - \Delta(b)$  for different principal quantum numbers  $n$  and channel  $(l-l')$ :  $n=3, l=0, l'=1$  (solid),  $n=3, l=1, l'=2$  (dash-dotted),  $n=5, l=0, l'=1$  (dash-double dotted),  $n=9, l=0, l'=1$  (dashed), and  $n=9, l=7, l'=8$  (dot-double dashed). Also shown is  $1 - bK_1(b)$  (dotted).

$$H_3(b) = b^2K_0(b) + (2b + b^3)K_1(b),$$

$$H_4(b) = (3b^2 + b^4)K_0(b) + (6b + 2b^3)K_1(b),$$

$$H_5(b) = (12b^2 + 2b^4)K_0(b) + (24b + 7b^3 + b^5)K_1(b),$$

⋮

$$H_q(b) = \sum_{k=0}^q b^k [h_0(q, k)K_0(b) + h_1(q, k)K_1(b)]. \quad (17)$$

Note that the numerical coefficients of the powers of  $b$  are line-independent. These numerical coefficients  $h_0$  and  $h_1$  are given analytically by the recursion relation:

$$h_j(q+2, k) = (q+1)h_j(q+1, k) + \theta(k-2)[h_j(q, k-2) - qh_j(q-1, k-2)], \quad j=0, 1 \quad (18)$$

and it is understood that  $h_j(q, k) = 0$  for  $k < 0$  or  $k > q$ . It is clear that  $h_0(q, k) = 0$  for odd  $k$  and  $h_1(q, k) = 0$  for even  $k$ . Special cases are  $h_0(q, 0) = \delta_{q0}$ ,  $h_0(q, 2) = \frac{(q-1)!}{2}$  for  $q > 2$ ,  $h_1(q, 1) = (q-1)!$  for  $q > 0$ . Using  $s_0 = 1$  and the relation [10]

$$Ki_2(z) = z[K_1(z) - Ki_1(z)] \quad (19)$$

we have

$$1 - \Delta(b) = [1 - bK_1(b)] - b(s_1 - 1)Ki_1(b)$$

$$- b^2 \sum_{i=2}^{n+n'+\lambda} s_i H_{i-2}(b). \quad (20)$$

Although one can get highly accurate *analytic* approximations for  $Ki_1(b)$  by using the series and asymptotic expansions in [10], in fact this term may be dropped because as we mentioned  $s_1 = 1$ . In Fig. 1 we plot the first term as a function of  $b$  (dotted lines), as well as the full  $1 - \Delta(b)$  term for vari-

ous  $n$  and channels  $(l, l')$ . This first term vanishes at  $b=0$  and the ST result is recovered for  $b \geq 5$  if we were to drop all other terms; however, the other terms ensure that the ST result is actually recovered only at substantially higher  $b$ . Both  $1-\Delta(b)$  and  $\frac{1-\Delta(b)}{b}$  vanish for  $b \rightarrow 0$  ( $\rho \rightarrow 0$ ). There is therefore no divergence at small impact parameters in PST. The graphs in Fig. 1 may be used to provide accurate values for the “relevant wave-function extent” cutoff used in ST. Of special interest is the case where the shielding length (typically the Debye length) is smaller than the wave-function extent.

Finally all terms involving  $F_{i-2}, i > 1$  vanish for  $b=0$  because of  $b^i$ . They may be written

$$b^2 \sum_{i=2}^{n+n'+\lambda} s_i H_{i-2}(b) = K_0(b) \sum_{i=1}^n v_{2i} b^{2i} + K_1(b) \sum_{i=1}^n v_{2i+1} b^{2i+1}, \quad (21)$$

where  $v_j$  are (line-dependent, because they involve the  $s_i$ ) numerical coefficients and we substituted  $n=n', \lambda=1$ . The series breaks up into two series, one involving  $K_0$  and even powers of  $b$  and the other  $K_1$  and odd powers of  $b$ . For large impact parameters  $K_1$  and  $K_0$  have an exponential decay and the ST result is recovered. The coefficients are given explicitly by

$$v_j = \sum_{k=j}^{n+n'+\lambda} s_k h(k-2, j-2) \quad (22)$$

with  $h$  being  $h_0$  for even and  $h_1$  for odd  $j=2, \dots, n+n'+\lambda$ . In particular,  $v_2=s_2=0.5$ . Evidently,  $v_2$  is also a line-independent term.

#### IV. IMPACT PARAMETER INTEGRATION

In the PST the expression for the final collision operator is reduced to one-dimensional quadratures:

$$\phi^{\text{PST}} = - \frac{4\pi e^4 n}{3(4\pi\epsilon_0 \hbar)^2} \sqrt{\frac{2m}{\pi kT}} \int_0^{b_{\max}} \frac{db}{b} \times [1 - \Delta(b; n_\alpha, l_\alpha, n_{\alpha'}, l_{\alpha'})][1 - \Delta(b; n_\alpha, l_{\alpha'}, n_\alpha, l_\alpha')] \quad (23)$$

for the noninterference terms, where  $\alpha$  refers to states of the upper or lower levels and  $b_{\max}$  refers to  $a\rho_{\max}$ , with  $a$  corresponding to the upper or lower level, respectively. For the interference terms, we have

$$\phi_i^{\text{PST}} = - \frac{8\pi e^4 n}{3(4\pi\epsilon_0 \hbar)^2} \sqrt{\frac{2m}{\pi kT}} \int_0^{b_{\max}} \frac{db}{b} \times [1 - \Delta(b; n_\alpha, l_\alpha, n_{\alpha'}, l_{\alpha'})] \times \left[ 1 - \Delta\left(\frac{n_\alpha b}{n_\beta}; n_\beta, l_{\beta'}, n_\beta, l_{\beta'}\right) \right], \quad (24)$$

where  $\alpha$  refers to states of the upper and  $\beta$  to the states of the lower levels. (Note that  $b$  is scaled for the lower level.)

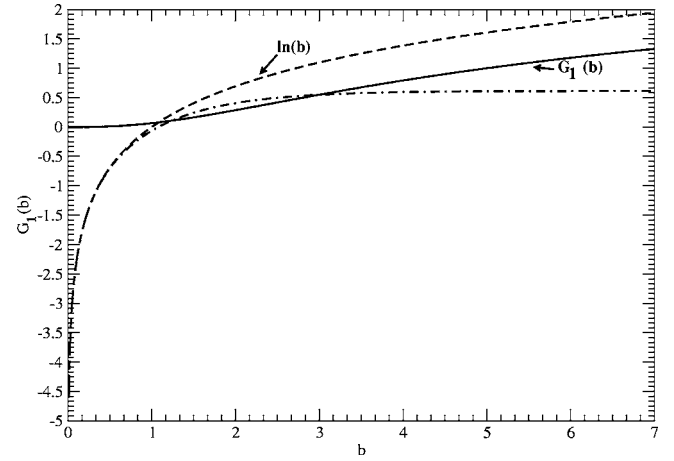


FIG. 2. The  $G_1$  function.

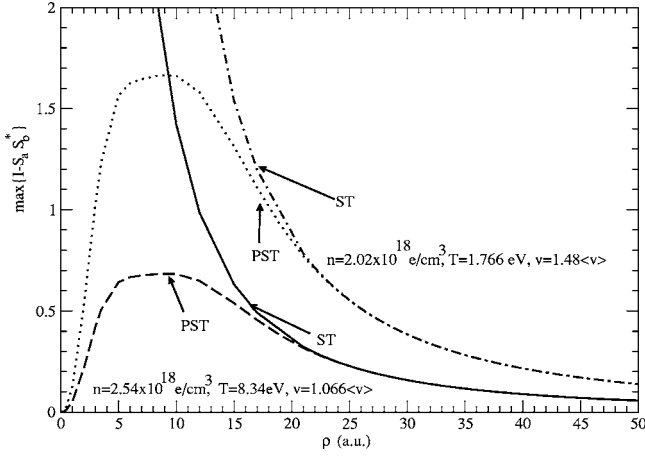
Here  $b_{\max}$  corresponds to the upper level's  $b_{\max}$ . The interference integral is a two-parameter function, with arguments  $b_{\max}, \frac{n_\alpha}{n_\beta}$ . These integrals are numerically easy to compute and tables may be given for any line. In view of the speed of modern computers, such tables appear unnecessary. Using the analytic form of  $\Delta(b)$  we identify the dominant contribution:

$$G_1(b_{\max}) = \int_0^{b_{\max}} \frac{db}{b} [1 - bK_1(b)]^2, \quad (25)$$

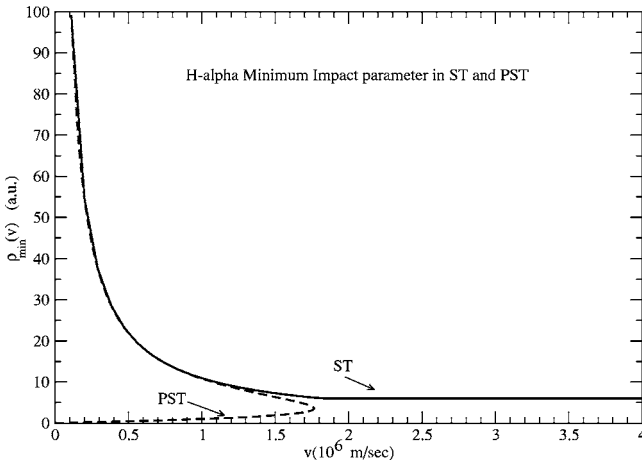
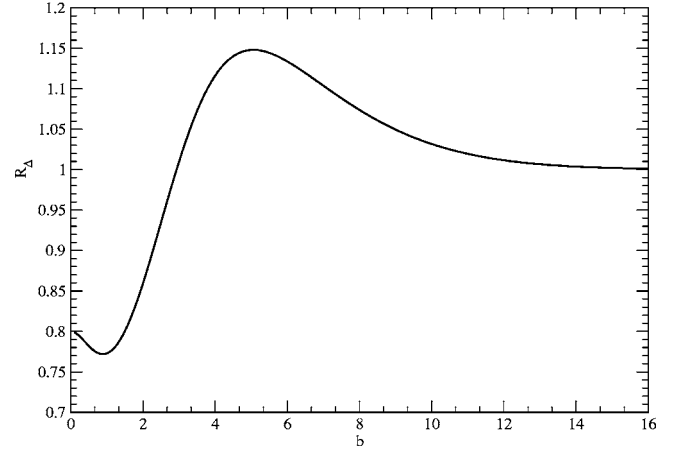
where  $b_{\max} = a\rho_{\max}$ . Figure 2 shows  $G_1(b)$  (solid line). Note that this term dominates for large  $b$ . Also shown in Fig. 2 are  $\ln(b)$  (dashed) and  $\ln(b) - G_1(b)$  (dash-dotted). It is interesting to note that concerning the ST result  $\ln(b_{\max}/b_{\min})$ , and the much discussed “exact” value of the strong collision constant, this difference may be taken as the *log* of “the” effective minimum impact parameter multiplied by  $a$ , provided of course we can neglect the other terms, which remain bound and hence contribute solely to the constant added to the logarithm (neglecting other sources of strong collisions, namely unitarity issues).

#### V. THE PST MINIMUM IMPACT PARAMETER

To summarize our theory: PST is convergent for all line components. However, being convergent does not make it necessarily right and we must address issues related to the validity of perturbation theory. It is interesting to note that in PST we also need a minimum impact parameter, but for a completely different reason: In PST for high enough velocities we can always integrate down to zero impact parameters. Unitarity of the perturbative second-order expressions is only violated for slow collisions. It is not violated for fast collisions, no matter what the impact parameter. In addition, at low velocities, unitarity is still satisfied for small enough impact parameters because of penetration. This means that the minimum impact parameter of ST,  $\rho_{\min}(v)$ , is not that simple anymore, as Fig. 3 illustrates for the maximum of the diagonal elements for the  $H_\alpha$  line of the quantity expanded via a second-order perturbation theory,

FIG. 3. Maximum diagonal matrix element of  $(I-S_{\alpha S} S_b^\dagger)$ .

i.e.,  $\{I-S_a(\rho, v)S_b^\dagger(\rho, v)\}$  versus impact parameter (in atomic units). Here  $S$  denotes the  $S$ -matrix, and the subscripts  $a$  and  $b$  correspond to the upper and lower levels, respectively. This quantity is plotted for two different velocities: The dotted (PST) and dash-dotted (ST) graphs correspond to a very low velocity, 1.48 times the average velocity,  $\langle v \rangle$  of a very cold plasma ( $T=1.76$  eV). We see that unitarity is satisfied [in the sense  $I-S_a(\rho, v)S_b^\dagger(\rho, v) \leq 1$ ] for  $\rho \leq 3$  and  $\rho > 17$  for PST. For the higher velocity case, namely  $v = 2.175\langle v \rangle$ , but with  $\langle v \rangle$  corresponding to an electron temperature of 8.34 eV, we see that in PST (dashed) unitarity is practically always satisfied for all impact parameters, whereas it breaks down for  $\rho \leq 11$  for ST (solid). The conclusion is that defining a velocity-dependent minimum impact parameter  $\rho_{min}(v)$ , as in ST, is not possible. Figure 4 shows the minimum impact parameter versus velocity for the  $H_\alpha$  line for ST (solid) and PST (dashed). The phase space region to the left of these curves corresponds to strong (more appropriately called “slow”) collisions. The main advantage of PST is the reduction of the strong collision phase space for large velocities. How important this will be depends on the importance of this region for the parameters of any particular experiment. This region could not be accurately estimated by ST due to penetration effects. Further-

FIG. 4. Plots of  $\rho_{min}(v)$ .FIG. 5. Variation of  $1-\Delta(b)$  with channel  $(l-l')$  for  $n=3$ . In this case we only have two channels ( $l=0-l'=1, l=1-l'=2$ ) and only one ratio  $R_\Delta$ .

more, ST usually completely dropped the contribution of this region to the interference terms, while PST also includes this contribution.

We mentioned that defining a velocity-dependent minimum impact parameter  $\rho_{min}(v)$  is not simple in PST because to a given  $v$ , there corresponds in general 0, 1, or 2 values of  $\rho_{min}(v)$ . On the other hand, it is simpler and advantageous to instead define a minimum impact-parameter-dependent velocity  $v_{min}(\rho)$  such that unitarity is satisfied for  $v \geq v_{min}(\rho)$ . The advantages of this approach, which is equivalent to the standard definition of a velocity-dependent minimum impact parameter, is not only computational, but also helps to remind us that *only slow collisions may be strong*. This means that  $\phi^{PST}$  is now given by

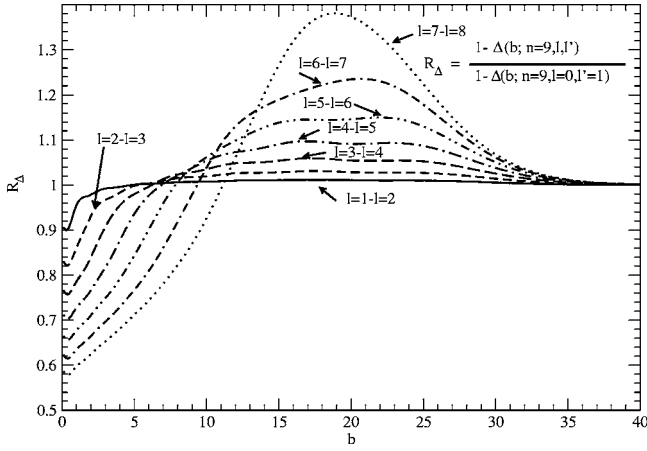
$$\begin{aligned} \phi^{PST} &= -\frac{4\pi e^4 n}{3(4\pi\epsilon_0\hbar)^2} \int_0^{b_{max}} \frac{db}{b} \int_{v_{min}}^{\infty} \frac{f(v)}{v} dv \\ &\quad \times [1 - \Delta(b; n_\alpha, l_\alpha, n_{\alpha'}, l_{\alpha'})]^2 \\ &= -\frac{4\pi e^4 n}{3(4\pi\epsilon_0\hbar)^2} \int_0^{b_{max}} \frac{db}{b} e^{-mv_{min}^2(b)/2kT} \\ &\quad \times [1 - \Delta(b; n_\alpha, l_\alpha, n_{\alpha'}, l_{\alpha'})]^2, \end{aligned} \quad (26)$$

with  $b_{max} = 2\rho_{max}/n_\alpha a_0$ , and similar terms for the lower level. The strong collision term (more precisely termed “slow collision term” in PST) is

$$\begin{aligned} &2\pi n \int_0^{\rho_{max}} \rho d\rho \int_0^{v_{min}(\rho)} v f(v) dv \\ &= 2\sqrt{\frac{8\pi kT}{m}} n \int_0^{\rho_{max}} \rho d\rho \int_0^{mv_{min}^2(\rho)/2kT} x e^{-x} dx \\ &= 2\sqrt{\frac{8\pi kT}{m}} n \int_0^{\rho_{max}} \rho d\rho (1 - e^{-X(\rho)} [1 + X(\rho)]) \end{aligned} \quad (27)$$

with  $X(\rho) = mv_{min}^2(\rho)/2kT$  corresponding to the assumption  $\{I-S_{\alpha S} S_\beta^\dagger\} = 1$ , which is now reasonable, as this quantity oscil-



FIG. 6. Variation of  $1-\Delta(b)$  with channel for  $n=9$ .

lates around unity when unitarity breaks down and we effectively use its average for the region where perturbation theory is not valid.

There remains to determine  $v_{min}(\rho)$ . This determination, as in the ST determination of  $\rho_{min}(v)$ , amounts to solving

$$\left(\frac{4e^2}{4\pi\epsilon_0\hbar a_0 v}\right)^2 \left[ \frac{r_{\alpha\alpha'}^2}{n_\alpha^2} \left( \frac{1-\Delta(b; n_\alpha, l_\alpha, n_{\alpha'}, l_{\alpha'})}{b} \right)^2 + \frac{r_{\beta\beta'}^2}{n_\beta^2} \left( \frac{1-\Delta(b'; n_\beta, l_\beta, n_{\beta'}, l_{\beta'})}{b'} \right)^2 - 2 \frac{\mathbf{r}_{\alpha\alpha'} \cdot \mathbf{r}_{\beta\beta'}}{n_\alpha n_\beta} \left( \frac{1-\Delta(b; n_\alpha, l_\alpha, n_{\alpha'}, l_{\alpha'})}{b} \right) \times \left( \frac{1-\Delta(b'; n_\beta, l_\beta, n_{\beta'}, l_{\beta'})}{b'} \right) \right] = 1. \quad (28)$$

Although this may be done separately for each matrix element [11], yielding a different  $v_{min}$  for each matrix element, we wish to keep the discussion on the same level as ST, which does not employ matrix element-dependent cut-

offs. Hence to be able to compare it to  $v_{min}^{ST}(\rho) = \frac{\hbar(n_a^2 - n_b^2)}{m\rho}$ , we determine  $v_{min}(\rho)$  as

$$v_{min}^{PST}(\rho) = \frac{2\hbar}{ma_0} \left[ n_a Z \left( \frac{2\rho}{n_a a_0} \right) - n_b Z \left( \frac{2\rho}{n_b a_0} \right) \right] \quad (29)$$

with

$$Z(b) = \frac{1}{n-1} \sum_{l=0}^{n-2} \frac{1-\Delta(b; n, l, l+1)}{b}, \quad (30)$$

which represents an average value for  $\frac{1-\Delta(b)}{b}$ . In Fig. 5 and 6 we plot the quantity  $R_\Delta = \frac{1-\Delta(b; n, l, l')}{1-\Delta(b; n, l=0, l'=1)}$  for  $n=3$  and  $n=9$  in order to illustrate the variation in  $1-\Delta(b)$  with channel ( $l-l'$ ). As mentioned above, this is only relevant if one wishes to use a  $v_{min}$  that is the same for each matrix element.

We note that  $v_{min}(\rho)$  is line-dependent, but does not depend on the plasma parameters (these determine how important this cutoff is in the weak-strong collision separation, i.e., the relative importance of the different regions of this graph). Therefore it may be given explicitly in closed form, thus further speeding up calculations (even though its computation is quite fast).

We must note here that for high-density plasmas, where the “strong”—or better, slow—collision term is important, the details of the cutoff  $v_{min}(\rho)$  are important. However, this is no different from the ST case and is not discussed any further here.

## VI. COMPARISON WITH EXPERIMENT

Part of the problem with high density ( $>10^{18}$  e/cm<sup>3</sup>) hydrogen experiments is the lack of data that may be considered “benchmark.” Even more problematic is the lack of well-diagnosed data in yet higher density ( $\geq 10^{20}$  e/cm<sup>3</sup>), where penetration effects could be even more dramatic. In Table I we compare ST and PST calculations with high density hydrogen experiments [12,13], discussed in detail in [14,15]. These calculations only include dipole terms and

TABLE I.  $H_\alpha$  Böddecker *et al.* [12] and Büscher *et al.* [13] data.

$n(10^{18}$ e/cm <sup>3</sup> )	$T(\text{eV})$	Expt.	ST	ST-weak	PST	PST-weak
2.44	7	153±21	75.3	55.25	61.5	60.2
3.44	7.6	182±24	100.16	70.84	79	77.55
4.84	8.4	187±36	133.5	90.3	101	99.2
7.08	9.2	228±64	184	118.5	132.96	130.8
9.27	10	245±54	231.16	143.2	160.9	158.5
0.49	5.77	40.3±4.3	20.35	16.5	17.88	17.56
0.53	10.46	45.4±3.8	21.22	15.75	16.5	16.4
0.68	6.39	47.4±6.5	26.5	21	22.74	22.36
0.99	7.12	53.1±6.5	36	27.67	30	29.52
1.35	7.82	67.8±2.5	46.42	34.7	37.6	37.1
1.96	8.4	81.9±5.6	63.2	45.72	49.8	49.1
2.54	8.34	96.2± 9.5	78.32	55.76	61.18	60.22

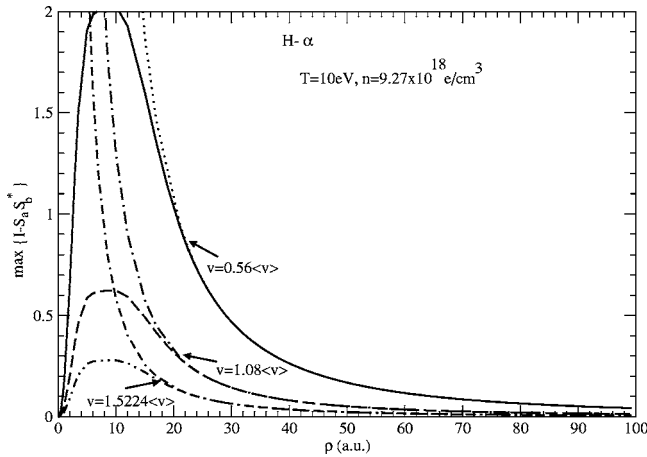


FIG. 7. Analysis of the PST vs ST differences for the highest density point of [12].

do not include any estimates of either quadrupole or inelastic contributions because we wish to avoid possible distortion of the comparisons due to differences in ST calculations and estimates. We show the ST and PST widths (full width at half maximum) in Å as well as the corresponding widths (ST-weak and PST-weak) with “weak” collisions only, i.e., with no strong collision term (equivalently  $\{I-S_a S_b^*\}=0$  for strong collisions). Note that PST gives a *larger* width for the “weak” collision contribution, but a much smaller strong collision term. This increases the relative proportion of the part of phase space that is reliably computed (“weak” collisions) compared to those estimated (strong collision term).

To understand the significant differences between the PST and ST calculations, it is instructive to look at the  $\{I-S_a S_b^*\}$  graphs of Fig. 7: Figure 1 shows that penetration is an issue for  $b \leq 10$ , i.e.,  $\rho \leq 15a_0$  for the upper level. For the plasma parameters in question the shielding length is about  $100a_0$ . Figure 7 shows the maximum  $\{I-S_a S_b^*\}$  matrix element as a function of impact parameter  $\rho$  for different velocities:  $v=0.56\langle v \rangle$  (solid for PST and dotted for ST),  $v=1.08\langle v \rangle$  (dashed for PST and dash-dotted for ST) and  $v=1.5\langle v \rangle$  (dash-double-dotted for PST and dot-double-dashed for ST). As expected, we see significant differences between PST and ST for  $\rho \leq 15a_0$ . However, we see that, for instance, for  $v \geq \langle v \rangle$ , the contribution of  $\rho \leq 15a_0$  to a strong collision term based on  $\{I-S_a S_b^*\}=1$  is overestimated in ST by at least a factor of 2. This means that whereas in this region ST has a problem with unitarity, in reality there is no such problem when penetration is accounted for, as in PST. In fact the region  $v \geq 0.7\langle v \rangle$ , for which unitarity is satisfied in PST, provides 82% of the width.

There remains to establish the importance of the  $\rho \leq 15a_0$  regime to the final ST width. As seen from the table, the strong collision term accounts for a substantial part of the total ST width, and only a very small part of the total PST width. This illustrates the importance of accounting for penetration in dense plasmas. With regard to the experimental results we note [14] important ion dynamical effects, especially for the lower densities,

not included in the calculations shown here, as well as experimental problems [15]. Further issues related to dense plasma hydrogen broadening are discussed in [11,16,17].

## VII. COMMENTS

In the Introduction we briefly commented on the so-called strong collisions. At least for hydrogen, it turns out that whether a collision is strong or not is basically determined by the velocity. Standard estimates [18] consider a collision as strong when the impact parameter is no larger than the Weisskopf radius, which is approximately  $\frac{\hbar(n_\alpha^2 - n_\beta^2)}{mv}$  with  $n_\alpha$  and  $n_\beta$  the upper and lower principal quantum numbers. If this is smaller than the wave-function extent, usually taken to be of the order of approximately  $n_\alpha^2 a_0$ , penetration is important and the collision is actually weak.

From Fig. 3 we see that PST’s advantage over ST arises mostly for temperatures that are not too low, combined with high densities. We see that the PST and ST differences are most important for the highest temperature. In the low temperature case ( $T=1.76$  eV), both ST and PST require a strong collision estimate ( $\{I-S_a S_b^*\}=1$ ) for  $\rho \leq 17a_0$  for  $v=1.48\langle v \rangle$ , except for an extremely small region  $\rho \leq 3a_0$  in PST. As a result, PST is not much more accurate than ST in that case, unless the shielding length is comparable to  $3a_0$ , i.e., smaller than the wave-function extent.

One of the long-standing issues in plasma spectroscopy is line merging and continuum lowering. A number of models have been presented, with Inglis-Teller [18] perhaps the best known. In essence [19] a number of effects occur in line merging: Because nearest neighbors come close compared to the wave-function extent of the bound electron, the potential felt by the electron is modified and eventually that electron can be found at no cost in energy much further away from its center, closer to the neighboring center. Eventually such an electron becomes a free plasma electron, as its wave function becomes delocalized over many centers. This mechanism is not different from the solid state picture. However, in hot plasmas the most powerful delocalization as well as localization mechanism is dynamic [19]: Due to collisions the bound wave function begins to spread and eventually will become macroscopic, unless it is recaptured. This is also the collisional (impact) picture of Stark broadening, which is at least a major contributor to the level broadening of levels close to the limit, and for which penetrating collisions can be important. In addition, far infrared and longer wavelength lines, which have a substantial wave-function extent, are of significant interest in astrophysics [20,21], though typically at low densities.

## APPENDIX: DERIVATION OF THE EXPRESSION FOR THE CORRECTION FACTOR

In

$$C_\lambda(R;n,l,n',l') = \frac{\int_0^{aR} dz e^{-z} z^{\lambda+l+l'+2} L_{n+l}^{2l+1}(z) L_{n'+l'}^{2l'+1}(z)}{\int_0^\infty dz e^{-z} z^{\lambda+l+l'+2} L_{n+l}^{2l+1}(z) L_{n'+l'}^{2l'+1}(z)} + (aR)^{2\lambda+1} \frac{\int_{aR}^\infty dz e^{-z} z^{-\lambda+l+l'+1} L_{n+l}^{2l+1}(z) L_{n'+l'}^{2l'+1}(z)}{\int_0^\infty dz e^{-z} z^{\lambda+l+l'+2} L_{n+l}^{2l+1}(z) L_{n'+l'}^{2l'+1}(z)} \quad (A1)$$

the  $L$  are the Laguerre polynomials:

$$L_{n+l}^{2l+1}(z) = \sum_{k=0}^{n-l-1} (-1)^{k+2l+1} \frac{[(n+l)!]^2 z^k}{(n-l-1-k)! (2l+1+k)! k!} \quad (A2)$$

The product of the Laguerre polynomials may then be written as

$$L_{n+l}^{2l+1}(z) L_{n'+l'}^{2l'+1}(z) = \sum_{p=0}^{n-l+n'-l'-2} a_p z^p \quad (A3)$$

with

$$a_p = \frac{[(n+l)! (n'+l')!]^2 (-1)^p}{\binom{\min(n-l-1,p)}{k=\max(0,p+1+l'-n')}} [(n-l-1-k)! (2l+1+k)! k! (n'-l'-1-p+k)! (2l'+1+p-k)! (p-k)!]^{-1} \quad (A4)$$

Note that because the factor  $[(n+l)! (n'+l')!]^2$  enters both the numerator and the denominator in  $C_\lambda$ , it may be dropped.

Therefore we have integrals of the type

$$\int dz e^{-z} z^k = -e^{-z} \sum_{m=0}^k \frac{k! z^{k-m}}{(k-m)!} \quad (A5)$$

and hence analytic expressions for  $C_\lambda$ :

$$C_\lambda(R;n,l,n',l') = I_1 + (aR)^{2\lambda+1} I_2 \quad (A6)$$

with

$$I_1 = \frac{\sum_{k=\lambda+l+l'+2}^{n+n'+\lambda} \left[ c_k k! \left( 1 - e^{-aR} \sum_{r=0}^k \frac{(aR)^{k-r}}{(k-r)!} \right) \right]}{\sum_{k=\lambda+l+l'+2}^{n+n'+\lambda} c_k k!} \quad (A7)$$

and

$$I_2 = \frac{\sum_{k=l+l'+1-\lambda}^{n+n'-\lambda-1} d_k e^{-aR} k! \sum_{r=0}^k \frac{(aR)^{k-r}}{(k-r)!}}{\sum_{k=\lambda+l+l'+2}^{n+n'+\lambda} c_k k!}, \quad (A8)$$

where

$$c_q = a_{q-\lambda-l-l'-2} \quad (A9)$$

and

$$d_k = a_{k+\lambda-1-l-l'}, \quad (A10)$$

so that

$$C_\lambda(R;n,l,n',l') = 1 - e^{-aR} \frac{\sum_{k=\lambda+l+l'+2}^{n+n'+\lambda} c_k k! \sum_{r=0}^k \frac{(aR)^{k-r}}{(k-r)!} - \sum_{k=l+l'+1-\lambda}^{n+n'-\lambda-1} d_k k! \sum_{r=0}^k \frac{(aR)^{2\lambda+1+k-r}}{(k-r)!}}{\sum_{k=\lambda+l+l'+2}^{n+n'+\lambda} c_k k!} \quad (A11)$$

In the second sum, setting  $k \rightarrow k+2\lambda+1$ , this may be written as



$$C_\lambda(R;n,l,n',l') = 1 - e^{-aR} \frac{\sum_{k=\lambda+l+l'+2}^{n+n'+\lambda} c_k \left[ k! \sum_{r=0}^k \frac{(aR)^{k-r}}{(k-r)!} - (k-2\lambda-1)! \sum_{r=0}^{k-2\lambda-1} \frac{(aR)^{k-r}}{(k-r-2\lambda-1)!} \right]}{\sum_{k=\lambda+l+l'+2}^{n+n'+\lambda} c_k k!}. \quad (\text{A12})$$

Clearly we can then write  $C_\lambda = 1 - e^{-aR} P_{n+n'+\lambda}(aR)$ , where  $P_k(x) = \sum_{i=0}^k s_i x^i$  is a polynomial of degree  $k$ . The coefficients  $s_i$  are

$$s_i = D^{-1} \left[ \sum_{j=\max(i,\lambda+l+l'+2)}^{n+n'+\lambda} \frac{c_j j!}{i!} - \theta(i-2\lambda-1) c_j \frac{(j-2\lambda-1)!}{(i-2\lambda-1)!} \right], \quad (\text{A13})$$

where we defined

$$D = \sum_{k=\lambda+l+l'+2}^{n+n'+\lambda} c_k k! \quad (\text{A14})$$

and  $\theta(j) = 1, j \geq 0$ , and 0 otherwise. Note that for  $i = n+n'+\lambda, s_i = 0$  because we have only the term  $j = i$ , since  $i = n+n'+\lambda \geq (l+1) + (l'+1) + \lambda$ .

- 
- [1] H. R. Griem, *Spectral Line Broadening by Plasmas* (Academic, New York, 1974).
- [2] K. Grützmacher and B. Wende, Phys. Rev. A **16**, 243 (1977).
- [3] T. Wujec, W. Olchawa, J. Halenka, and J. Musielok, Phys. Rev. E **66**, 066403 (2002).
- [4] M. L. Adams, R. W. Lee, H. A. Scott, H. K. Chung, and L. Klein, Phys. Rev. E **66**, 066413 (2002).
- [5] S. Alexiou and R. W. Lee, in *Spectral Line Shapes*, edited by J. Seidel, AIP Conf. Proc. No. 599 (AIP, Melville, NY, 2001), pp. 135–143.
- [6] S. Alexiou and R. W. Lee, J. Quant. Spectrosc. Radiat. Transf. (to be published).
- [7] S. Alexiou, in *Spectral Line Shapes*, edited by C. Back, AIP Conf. Proc. No. 645 (AIP, Melville, NY, 2002), pp. 302–309.
- [8] D. B. Boercker and C. A. Iglesias, Phys. Rev. A **30**, 2771 (1984).
- [9] S. Alexiou, J. Quant. Spectrosc. Radiat. Transf. **81**, 13 (2003).
- [10] M. Abramowitz and I. Stegun, *Handbook of Mathematical Functions* (Dover, New York, 1974).
- [11] S. Alexiou, J. Quant. Spectrosc. Radiat. Transf. (to be published).
- [12] S. Böddeker, S. Gönter, A. Könies, L. Hitzschke, and H. J. Kunze, Phys. Rev. E **47**, 2785 (1993).
- [13] S. Büscher, Th. Wrubel, S. Ferri, and H. J. Kunze, J. Phys. B **35**, 2889 (2002).
- [14] S. Alexiou, Phys. Rev. E **71**, 066403 (2005).
- [15] S. Alexiou and E. Leboucher-Dalimier, Phys. Rev. E **60**, 3436 (1999).
- [16] H. R. Griem, J. Halenka, and W. Olchawa, J. Phys. B **28**, 975 (2005).
- [17] S. Alexiou, H. R. Griem, J. Halenka, and W. Olchawa, J. Quant. Spectrosc. Radiat. Transf. (to be published).
- [18] H. R. Griem, *Plasma Spectroscopy* (McGraw-Hill, New York, 1964).
- [19] J. Stein, J. Quant. Spectrosc. Radiat. Transf. **54**, 395 (1995).
- [20] M. Carlsson and R. J. Rutten, Astron. Astrophys. **259**, L53 (1992).
- [21] O. Motapon and N. Minh, Astron. Astrophys., Suppl. Ser. **139**, 377 (1999).